

***CP* violating mode of the stoponium decay into Zh** Kingman Cheung^{1,2,3}, Wai-Yee Keung⁴, Po-Yan Tseng⁵¹ *National Center for Theoretical Sciences, Hsinchu, Taiwan*² *Department of Physics, National Tsing Hua University, Hsinchu 300, Taiwan*³ *Division of Quantum Phases & Devices, School of Physics,
Konkuk University, Seoul 143-701, Republic of Korea*⁴ *Department of Physics, University of Illinois at Chicago, Illinois 60607 USA*⁵ *Kavli IPMU (WPI), UTIAS, The University of Tokyo, Kashiwa, Chiba 277-8583, Japan*

(Dated: April 12, 2018)

Abstract

We show that a novel decay mode Zh of the bound state of stop-anti-stop pair in the ground state $^1S_0(\tilde{t}_1\tilde{t}_1^*)$ may have a significant branching ratio if the CP violating mixing appears in the stop sector, even after we apply the stringent constraint from the measurement of the electric dipole moment (EDM) of the electron. We show that the branching ratio can be as large as 10% in some parameter space that it may be detectable at the LHC.

I. INTRODUCTION

So far the Higgs boson discovered in 2012 is the only fundamental particle of scalar in nature [1]. On the other hand, colored scalar bosons are definitely signs of physics beyond the standard model (SM), which often appears in many new physics models. One outstanding example is the scalar-top (stop) quark – superpartner of the top quark – in the Minimal Supersymmetric Standard Model (MSSM). Their strong interaction allows them to be produced abundantly at hadron colliders if kinematically allowed. The current search for the stop at LHC has pushed its mass above about 500 GeV [2]. To escape its detection, the mass of the lightest stop state \tilde{t}_1 is compressed just above the lightest neutralino mass so that there is not much missing momentum for tagging the event at the LHC. In such a scenario, the stop state is rather long lived in comparison to the time scale of QCD hadronization. Therefore, the stop-anti-stop pair can form the bound state, called the stoponium[3], which is produced through the gluon-gluon fusion [3–5] as in the squarkonium[6] production. The ground state $\tilde{\eta} \equiv {}^1S_0(\tilde{t}_1\tilde{t}_1^*)$ of the stoponium can then be identified by its distinctive decay modes, such as hh , WW , ZZ , $\gamma\gamma$, etc. Among them, the channel hh stands out[3] for its significant decay rate with clean detection signature. Recent studies of the stoponium at LHC can be found in [7–12]. There are also efforts in studying the QCD corrections [13, 14], the lattice calculation[15], the mixing between the Higgs boson and the stoponium[16], and the role of the stoponium[17] in the dark matter co-annihilation.

Surprisingly in all studies about the stoponium decay, the channel Zh is not given. In fact, the process is forbidden by the underlying assumption of the CP conservation, which implies the cancellation of amplitudes á la the Furry theorem. However, there is no strong argument against CP violation in the stop sector. We are going to show in this article that $\tilde{\eta} \rightarrow hZ$ can have a significant branching ratio when CP violating parameters are chosen yet within the experimental constraint due to the electron electric dipole moment (eEDM) measurement.

If the mass of the stoponium is close to the mass m_A of the pseudoscalar Higgs boson, substantial enhancement of the Zh decay mode happens due to the resonance effect. Nevertheless, for a stoponium mass around 1.2 TeV $\sim m_A$ the eEDM places a very stringent constraint on the choice of the CP -violating parameter such that the $B(\tilde{\eta} \rightarrow Zh) \sim 10^{-3}$. On the other hand, if the mass of the second stop is not too far from the lightest stop,

substantial cancellation between the stop contributions to the eEDM can happen, such that the CP -violating parameter can be chosen to be much larger and the branching ratio $B(\tilde{\eta} \rightarrow Zh) \sim 10^{-1}$. In the extreme case that the $m_A \rightarrow \infty$ when the eEDM is not effective, the branching ratio can reach a large value, $B(\tilde{\eta} \rightarrow Zh) \sim O(0.5)$. This is the major result of our work. Furthermore, due to the heavy stoponium decay the Z and h bosons are very boosted, in which both bosons can be identified as boosted objects with advanced boost techniques to suppress backgrounds. Such rather straightforward detection of the Z and h bosons makes the mode Zh a wonderful place to look for the new particle as well as CP violation.

The organization is as follows. In the next section, we give details about the mixing in the stop sector, as well as the CP -violating couplings to the Higgs boson and Z boson. In Sec. III, we analyze the decay mode Zh together with the eEDM constraint. In Sec. IV, we estimate the observability of the Zh mode at the LHC. We summarize in Sec. V.

II. CP -VIOLATION IN THE STOP SECTOR

Let us start with the Z boson couplings to the stops $t_i (i = 1, 2)$. The convective current among stop states is

$$J_{ij}^\mu = i\tilde{t}_i^* \overset{\leftrightarrow}{\partial} \tilde{t}_j \quad \text{where} \quad \overset{\leftrightarrow}{\partial} \equiv \overset{\rightarrow}{\partial} - \overset{\leftarrow}{\partial} .$$

Our convention for the Feynman vertex amplitude is

$$\langle \tilde{t}_i(p_i) | J_{ij}^\mu | \tilde{t}_j(p_j) \rangle = (p_j + p_i)^\mu ,$$

for the incoming p_j and the outgoing p_i . Under the charge conjugation C , $\tilde{t}_i \xrightarrow{C} \tilde{t}_i^*$. So $J_{ij}^\mu \xrightarrow{C} -J_{ji}^\mu$. The negative sign in the transformation of J comes from that in $\overset{\leftrightarrow}{\partial}$. Consequently, we need to make the C -odd transformation for the Z gauge boson, $Z^\mu \xrightarrow{C} -Z^\mu$. The hermiticity of the unitary interaction $\mathcal{L} \supset \sum_{ij} g_{ij}^Z J_{ij}^\mu Z_\mu$ requires $g_{ij}^Z = g_{ji}^{Z*}$. If the charge conjugation is a good symmetry, we have $g_{ij}^Z = g_{ji}^Z$. From this, we know that a complex g_{ij}^Z (for $i \neq j$) if its phase is not removable implies C -parity violation

In general, if the states $\tilde{t}_{L,R}$ mix with each other by the complex 2×2 matrix into the mass eigenstates $\tilde{t}_{1,2}$, we expect the complex off-diagonal g_{12}^Z coupling to the Z boson. However, we can set g_{12}^Z real by redefining the relative phase between the two stop fields \tilde{t}_1, \tilde{t}_2 . Indeed

in the next section, we adopt such a choice in our convention. To have a genuine C -parity non-conservation, we need additional complex coupling coefficient y , which appears in the Higgs vertex of $yh(\tilde{t}_2^*\tilde{t}_1)$. Then there is no more freedom to remove its phase.

For the renormalizable interaction of the pure bosonic sector, operators of dim 4 or less do not involve the P -odd Levi-Civita ϵ -symbol. Therefore, the P -parity is conserved in the Z vertex. Consequently, the C -parity violation is the CP -violation. Our example is the decay of the ground state of the stoponium in $^1S_0(\tilde{t}_1\tilde{t}_1^*)$ into Zh . The exchange of \tilde{t}_2 can appear in the t -channel and in the u -channel, as shown in the first two diagrams in Fig. 1. The phase of g_{ij}^Z is tied with another vertex $yh\tilde{t}_1^*\tilde{t}_2$, and thus overall unremovable. The two amplitudes of the u and t channels cancel if the coupling factor is real, but add up if imaginary. The production of Zh from such a decay is a sign of CP -violation.

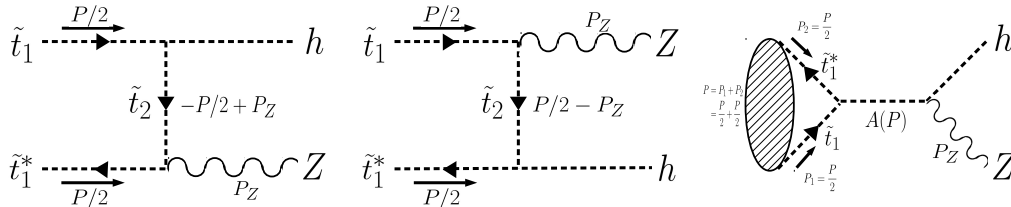


FIG. 1. Feynman diagrams for the stoponium decaying into Zh via the t, u, s channels from the left to the right.

Furthermore, there exists the direct coupling of the pseudoscalar A^0 to the stops, $A^0(\tilde{t}_1^*\tilde{t}_1 - \tilde{t}_2^*\tilde{t}_2)$, which is CP -violating. The ground state of the stoponium $\tilde{\eta}$ can annihilate into the virtual A^0 in the s -channel as in the third diagram in Fig. 1, and then become Zh via the ZA^0h gauge vertex. If the mass of the stoponium is close to the mass m_A of the pseudoscalar Higgs boson, substantial enhancement of the Zh decay mode happens, indeed the Zh mode is significant in such a scenario. Nevertheless, it is restricted by the eEDM especially when the mass eigenstates of the stop sector is widely separated and m_A is moderate. When m_A is chosen to be very heavy, then the constraint of eEDM disappears and the CP parameter can be chosen very large and the branching ratio into Zh can be as large as $O(0.5)$.

A. Complex mixing in the Stop sector

Input parameters in the calculation of the $\tilde{\eta} \rightarrow Zh$ decay mode include masses $m_{\tilde{t}_1}, m_{\tilde{t}_2}$, mixing parameters $\theta_{\tilde{t}}, \delta_u, \text{Re}[\mu^* e^{-i\delta_u}], \text{Im}[\mu^* e^{-i\delta_u}]$, and $\tan \beta$ is the ratio of the VEV of the two Higgs doublet.

The relative phase between the μ parameter and the trilinear A_t parameter can be established in the following $\tilde{t}_L \tilde{t}_R^*$ term in the Lagrangian:

$$\mathcal{L} \supset -y_t A_t \tilde{t}_L \tilde{t}_R^* H_u^0 + y_t \mu^* \tilde{t}_L \tilde{t}_R^* H_d^{0*} + H.c. + \dots, \quad (1)$$

where $y_t = \frac{\sqrt{2}m_t}{v \sin \beta}$, $v = 246$ GeV, and

$$\begin{aligned} H_u^0 &= \frac{1}{\sqrt{2}} [v s_\beta + (c_\alpha h + s_\alpha H) + i(A^0 c_\beta - G^0 s_\beta)], \\ H_d^0 &= \frac{1}{\sqrt{2}} [v c_\beta + (-s_\alpha h + c_\alpha H) + i(A^0 s_\beta + G^0 c_\beta)], \end{aligned} \quad (2)$$

where c_β, s_β are shorthand notation for $\cos \beta$ and $\sin \beta$, c_α, s_α are for $\cos \alpha$ and $\sin \alpha$, respectively, $\tan \beta \equiv v_u/v_d$ is the ratio of the VEV of the two Higgs doublet, and α is the mixing angle between the two neutral components of the Higgs doublets.

The stop mass matrix can be expressed as

$$(\tilde{t}_L^*, \tilde{t}_R^*) \begin{pmatrix} m_t^2 + M_Q^2 + m_Z^2(\frac{1}{2} - \frac{2}{3}x_W) \cos(2\beta) & m_t(A_t^* - \mu \cot \beta) \\ m_t(A_t - \mu^* \cot \beta) & m_t^2 + M_U^2 + m_Z^2(\frac{2}{3}x_W) \cos(2\beta) \end{pmatrix} \begin{pmatrix} \tilde{t}_L \\ \tilde{t}_R \end{pmatrix}.$$

We can define a phase δ_u by

$$A_t - \mu^* \cot \beta = |A_t - \mu^* \cot \beta| e^{i\delta_u}, \quad (3)$$

then the mass matrix can be diagonalized by an orthogonal transformation with an angle $\theta_{\tilde{t}}$ into mass eigenstates \tilde{t}_1 and \tilde{t}_2 :

$$\begin{pmatrix} \tilde{t}_L \\ \tilde{t}_R \end{pmatrix} = \begin{pmatrix} 1 & 0 \\ 0 & e^{i\delta_u} \end{pmatrix} \begin{pmatrix} \cos \theta_{\tilde{t}} & -\sin \theta_{\tilde{t}} \\ \sin \theta_{\tilde{t}} & \cos \theta_{\tilde{t}} \end{pmatrix} \begin{pmatrix} \tilde{t}_1 \\ \tilde{t}_2 \end{pmatrix}.$$

The stop mass matrix can be re-expressed in terms of $m_{\tilde{t}_1}, m_{\tilde{t}_2}, \theta_{\tilde{t}}$, and δ_u as

$$(\tilde{t}_L^*, \tilde{t}_R^*) \begin{pmatrix} m_{\tilde{t}_1}^2 \cos^2 \theta_{\tilde{t}} + m_{\tilde{t}_2}^2 \sin^2 \theta_{\tilde{t}} & e^{-i\delta_u} (m_{\tilde{t}_1}^2 - m_{\tilde{t}_2}^2) \sin \theta_{\tilde{t}} \cos \theta_{\tilde{t}} \\ e^{i\delta_u} (m_{\tilde{t}_1}^2 - m_{\tilde{t}_2}^2) \sin \theta_{\tilde{t}} \cos \theta_{\tilde{t}} & m_{\tilde{t}_1}^2 \sin^2 \theta_{\tilde{t}} + m_{\tilde{t}_2}^2 \cos^2 \theta_{\tilde{t}} \end{pmatrix} \begin{pmatrix} \tilde{t}_L \\ \tilde{t}_R \end{pmatrix}.$$

By comparing the off-diagonal elements of the above two stop mass matrix, we can express A_t in terms of $\text{Re}[\mu^* e^{-i\delta_u}]$, and $\text{Im}[\mu^* e^{-i\delta_u}]$:

$$\begin{aligned}\text{Re}[A_t e^{-i\delta_u}] &= \text{Re}[\mu^* e^{-i\delta_u}] \cot \beta + \left(\frac{m_{\tilde{t}_1}^2 - m_{\tilde{t}_2}^2}{m_t} \right) \sin \theta_{\tilde{t}} \cos \theta_{\tilde{t}}, \\ \text{Im}[A_t e^{-i\delta_u}] &= \text{Im}[\mu^* e^{-i\delta_u}] \cot \beta.\end{aligned}\quad (4)$$

B. Relevant Couplings for Zh decay mode

The interaction between h and $\tilde{t}_{L,R}$ is

$$\begin{aligned}\mathcal{L} &\subset h(\tilde{t}_L^*, \tilde{t}_R^*) \begin{pmatrix} V_{LL} & V_{LR}^* \\ V_{LR} & V_{RR} \end{pmatrix} \begin{pmatrix} \tilde{t}_L \\ \tilde{t}_R \end{pmatrix} \\ &= h(\tilde{t}_L^*, \tilde{t}_R^*) \begin{pmatrix} -\frac{gm_t^2 c_\alpha}{m_W s_\beta} + \frac{gm_Z}{\sqrt{1-x_W}} \left(\frac{1}{2} - \frac{2}{3}x_W\right) s_{\alpha+\beta} & -\frac{1}{2} \frac{gm_t}{m_W s_\beta} (A_t^* c_\alpha + \mu s_\alpha) \\ -\frac{1}{2} \frac{gm_t}{m_W s_\beta} (A_t c_\alpha + \mu^* s_\alpha) & -\frac{gm_t^2 c_\alpha}{m_W s_\beta} + \frac{gm_Z}{\sqrt{1-x_W}} \left(\frac{2}{3}x_W\right) s_{\alpha+\beta} \end{pmatrix} \begin{pmatrix} \tilde{t}_L \\ \tilde{t}_R \end{pmatrix} \\ &\equiv h(\tilde{t}_1^*, \tilde{t}_2^*) \begin{pmatrix} y_{\tilde{t}_1 \tilde{t}_1}^h & y_{\tilde{t}_1 \tilde{t}_2}^{h*} \\ y_{\tilde{t}_1 \tilde{t}_2}^h & y_{\tilde{t}_2 \tilde{t}_2}^h \end{pmatrix} \begin{pmatrix} \tilde{t}_1 \\ \tilde{t}_2 \end{pmatrix},\end{aligned}\quad (5)$$

where $m_W = \frac{g}{2}v$, $m_Z = \frac{1}{2}\sqrt{g^2 + g'^2}v$, $m_Z = m_W/\sqrt{1-x_W}$, and

$$\begin{aligned}y_{\tilde{t}_1 \tilde{t}_1}^h &= V_{LL} c_{\theta_{\tilde{t}}}^2 + V_{RR} s_{\theta_{\tilde{t}}}^2 + 2s_{\theta_{\tilde{t}}} c_{\theta_{\tilde{t}}} \text{Re}[V_{LR} e^{-i\delta_u}] \\ y_{\tilde{t}_2 \tilde{t}_2}^h &= V_{LL} s_{\theta_{\tilde{t}}}^2 + V_{RR} c_{\theta_{\tilde{t}}}^2 - 2s_{\theta_{\tilde{t}}} c_{\theta_{\tilde{t}}} \text{Re}[V_{LR} e^{-i\delta_u}] \\ y_{\tilde{t}_1 \tilde{t}_2}^h &= s_{\theta_{\tilde{t}}} c_{\theta_{\tilde{t}}} (V_{RR} - V_{LL}) + (c_{\theta_{\tilde{t}}}^2 - s_{\theta_{\tilde{t}}}^2) \text{Re}[V_{LR} e^{-i\delta_u}] + i \text{Im}[V_{LR} e^{-i\delta_u}],\end{aligned}\quad (6)$$

and

$$\begin{aligned}\text{Re}[V_{LR} e^{-i\delta_u}] &= -\frac{1}{2} \frac{gm_t}{m_W} \left\{ \frac{\cos(\beta - \alpha)}{s_\beta^2} \text{Re}[\mu^* e^{-i\delta_u}] + \frac{c_\alpha}{s_\beta} \left(\frac{m_{\tilde{t}_1}^2 - m_{\tilde{t}_2}^2}{m_t} \right) \sin \theta_{\tilde{t}} \cos \theta_{\tilde{t}} \right\}, \\ \text{Im}[V_{LR} e^{-i\delta_u}] &= -\frac{1}{2} \frac{gm_t}{m_W} \left\{ \frac{\cos(\beta - \alpha)}{s_\beta^2} \text{Im}[\mu^* e^{-i\delta_u}] \right\}.\end{aligned}\quad (7)$$

For the interaction between the heavy Higgs H and stops $\tilde{t}_{1,2}$, we need to change the above $h, \tilde{t}_{1,2}$ interactions by substitutions

$$h \longrightarrow H, \quad c_\alpha \longrightarrow s_\alpha, \quad -s_\alpha \longrightarrow c_\alpha.\quad (8)$$

On the other hand, the interaction between A^0 and $\tilde{t}_{L,R}$ is

$$\begin{aligned}
\mathcal{L} &\supset -\frac{im_t}{v \sin \beta} A^0(\tilde{t}_L^*, \tilde{t}_R^*) \begin{pmatrix} 0 & -(A_t^* c_\beta + \mu^* s_\beta) \\ A_t c_\beta + \mu^* s_\beta & 0 \end{pmatrix} \begin{pmatrix} \tilde{t}_L \\ \tilde{t}_R \end{pmatrix} \\
&= \frac{m_t}{v \sin \beta} A^0(\tilde{t}_1^*, \tilde{t}_2^*) \begin{pmatrix} 2s_{\theta_t} c_{\theta_t} \text{Im}[\hat{A}_t] & i(c_{\theta_t}^2 \hat{A}_t^* + s_{\theta_t}^2 \hat{A}_t) \\ -i(c_{\theta_t}^2 \hat{A}_t + s_{\theta_t}^2 \hat{A}_t^*) & -2s_{\theta_t} c_{\theta_t} \text{Im}[\hat{A}_t] \end{pmatrix} \begin{pmatrix} \tilde{t}_1 \\ \tilde{t}_2 \end{pmatrix} \\
&\equiv A^0(\tilde{t}_1^*, \tilde{t}_2^*) \begin{pmatrix} y_{\tilde{t}_1 \tilde{t}_1}^A & y_{\tilde{t}_1 \tilde{t}_2}^{A^*} \\ y_{\tilde{t}_1 \tilde{t}_2}^A & y_{\tilde{t}_2 \tilde{t}_2}^A \end{pmatrix} \begin{pmatrix} \tilde{t}_1 \\ \tilde{t}_2 \end{pmatrix}
\end{aligned} \tag{9}$$

where $\hat{A}_t \equiv (A_t c_\beta + \mu^* s_\beta) e^{-i\delta_u}$, and $\text{Im}[\hat{A}_t] = \text{Im}[\mu^* e^{-i\delta_u}] / \sin \beta$. Also, $y_{\tilde{t}_1 \tilde{t}_1}^A = -y_{\tilde{t}_2 \tilde{t}_2}^A$.

The interaction between Z boson and $\tilde{t}_{L,R}$ is

$$\begin{aligned}
\mathcal{L} &\supset \frac{g}{\sqrt{1-x_W}} Z^\mu(\tilde{t}_L^*, \tilde{t}_R^*) i \overleftrightarrow{\partial}_\mu \begin{pmatrix} -\frac{1}{2} + Q_t x_W & 0 \\ 0 & Q_t x_W \end{pmatrix} \begin{pmatrix} \tilde{t}_L \\ \tilde{t}_R \end{pmatrix} \\
&= \frac{g}{\sqrt{1-x_W}} Z^\mu(\tilde{t}_1^*, \tilde{t}_2^*) i \overleftrightarrow{\partial}_\mu \begin{pmatrix} -\frac{1}{2} c_{\theta_t} + Q_t x_W & \frac{1}{2} s_{\theta_t} c_{\theta_t} \\ \frac{1}{2} s_{\theta_t} c_{\theta_t} & -\frac{1}{2} s_{\theta_t}^2 + Q_t x_W \end{pmatrix} \begin{pmatrix} \tilde{t}_1 \\ \tilde{t}_2 \end{pmatrix} \\
&\equiv Z^\mu(\tilde{t}_1^*, \tilde{t}_2^*) i \overleftrightarrow{\partial}_\mu \begin{pmatrix} g_{\tilde{t}_1 \tilde{t}_1}^Z & g_{\tilde{t}_1 \tilde{t}_2}^Z \\ g_{\tilde{t}_1 \tilde{t}_2}^Z & g_{\tilde{t}_2 \tilde{t}_2}^Z \end{pmatrix} \begin{pmatrix} \tilde{t}_1 \\ \tilde{t}_2 \end{pmatrix},
\end{aligned} \tag{10}$$

where the two-way derivative $i \overleftrightarrow{\partial}_\mu$ applies only to the stop fields, and picks up $(p - p')_\mu$ of the stop momenta p, p' flowing into the vertex in the Feynman diagram.

The process $\tilde{t}_1 \tilde{t}_1^* \rightarrow hZ$ involve the s -channel diagram going by the A^0 exchange, as well as the t -channel and the conjugated u -channel by the \tilde{t}_2 exchange, as shown in Fig. 1.

In the non-relativistic approximation, the overall amplitude is

$$\mathcal{M}(\tilde{t}_1 \tilde{t}_1^* \rightarrow hZ) = - \left[\frac{4i \text{Im}(g_{\tilde{t}_1 \tilde{t}_2}^{Z^*} y_{\tilde{t}_1 \tilde{t}_2}^h)}{m_h^2 + m_Z^2 - 2(m_{\tilde{t}_1}^2 + m_{\tilde{t}_2}^2)} + \frac{2y_{\tilde{t}_1 \tilde{t}_1}^A g_{Ah}^Z}{4m_{\tilde{t}_1}^2 - m_A^2} \right] (P \cdot \varepsilon_Z), \tag{11}$$

where $g_{Ah}^Z = \frac{g}{2\sqrt{1-x_W}} \cos(\beta - \alpha)$. The overall transition rate requires the polarization sum,

$$\sum_{\varepsilon_Z} (P \cdot \varepsilon_Z)^2 = P^\mu \left(-g_{\mu\nu} + \frac{p_{Z\mu} p_{Z\nu}}{m_Z^2} \right) P^\nu = \frac{\lambda(s, m_h^2, m_Z^2)}{4m_Z^2}.$$

Here we use $2P \cdot p_Z = s + m_Z^2 - m_h^2$ and $s = m_\eta^2 \simeq 4m_{\tilde{t}_1}^2$. The kinematic function $\lambda(a, b, c) = a^2 + b^2 + c^2 - 2(ab + ac + bc)$. Note that all amplitudes are suppressed by the non-alignment factor $\cos(\beta - \alpha)$, which appears in both g_{Ah}^Z and $\text{Im}[y_{\tilde{t}_1 \tilde{t}_2}^h] = \text{Im}[V_{LR} e^{-i\delta_u}]$.

The partial decay width in the non-relativistic approximation is

$$\Gamma(\tilde{t}_1\tilde{t}_1^* \rightarrow hZ) = \frac{1}{(2m_{\tilde{t}_1})^2} \sum_{\varepsilon_Z} |\mathcal{M}(\tilde{t}_1\tilde{t}_1^* \rightarrow hZ)|^2 |\psi(0)|^2 \frac{3}{8\pi} \lambda^{\frac{1}{2}}(1, m_h^2/s, m_Z^2/s),$$

where the bound state wave function at the origin is estimated by the Coulomb type expression,

$$|\psi(0)|^2 = \frac{1}{27\pi} (\alpha_s 2m_{\tilde{t}_1})^3.$$

In comparison, we show the partial decay width of the gluon-gluon mode .

$$\Gamma(\tilde{t}_1\tilde{t}_1^* \rightarrow gg) = \frac{4\pi\alpha_s^2}{3m_{\tilde{t}_1}^2} |\psi(0)|^2.$$

C. Contributions to the Electron EDM

The most recent eEDM gives a very stringent constraint[18]

$$|d_e| < 8.7 \times 10^{-29} e \cdot [\text{cm}], \text{ at 90\% C.L.} \quad (12)$$

In MSSM, the relevant contribution to the eEDM based on the CP violating parameters in the stop sector $\tilde{t}_{1,2}$ arises via the two-loop Barr-Zee diagrams [19].

$$\left(\frac{d_e}{e}\right)_{2\text{-loop}}^{\tilde{t}} = 2Q_e Q_t^2 \frac{3\alpha_{\text{em}}}{64\pi^3} \frac{m_e}{m_A^2} \left(\frac{\sin 2\theta_{\tilde{t}} m_t \text{Im}[\mu^* e^{-i\delta_u}]}{v^2 \sin \beta \cos \beta} \right) \left[F\left(\frac{m_{\tilde{t}_1}^2}{m_A^2}\right) - F\left(\frac{m_{\tilde{t}_2}^2}{m_A^2}\right) \right], \quad (13)$$

where $\alpha_{\text{em}} = e^2/(4\pi)$, $v \simeq 246$ GeV, and $F(z)$ is a two-loop function given by

$$F(z) = \int_0^1 dx \frac{x(1-x)}{z-x(1-x)} \ln \left[\frac{x(1-x)}{z} \right]. \quad (14)$$

In fact the eEDM contribution vanishes in two different limits, first when A^0 becomes heavy and decoupled, and second when $m_{\tilde{t}_1} \simeq m_{\tilde{t}_2}$ so that their effects cancel each other. Our numerical results show that even in general cases, an ample parameter space satisfies the eEDM constraint, but still gives significant branching ratio mode of hZ .

Although the one-loop contributions to the eEDM 1-loop also exist in the neutralino-selectron diagram, and the chargino-sneutrino diagram, they involve totally different CP violating parameters and can be tuned to give tiny eEDM [20]. Therefore, we ignore their one-loop effect in eEDM. In another approach [21, 22], one can allow the sole contribution of one type of diagrams to exceed the current experimental limit, where one can expect that there might be other types of diagrams that would cancel one another.

III. ANALYSIS

The input parameters that are relevant for the stoponium decay into Zh are: $m_{\tilde{t}_1}$, $m_{\tilde{t}_2}$, $\text{Re}[\mu^* e^{-i\delta_u}]$, $\text{Im}[\mu^* e^{-i\delta_u}]$, $\theta_{\tilde{t}}$, $\tan\beta$, and m_A . In the computation of the branching ratios of the stoponium, it also involves the gluino mass $m_{\tilde{g}}$ and $\cos(\beta - \alpha)$.

Since we expect the pseudoscalar resonance can enhance the decay rate when $m_{\tilde{\eta}}$ is around the heavy pseudoscalar A^0 mass, we study the following cases,

1. Near and below the pole, $m_{\tilde{\eta}} < m_A$ by setting $2m_{\tilde{t}_1} = 1200$ GeV and $m_A = 1.5$ TeV.
2. Well below the pole, $m_{\tilde{\eta}} \ll m_A$ by setting $2m_{\tilde{t}_1} = 1200$ GeV and $m_A = 2.5$ TeV.
3. Far from the pole for an extremely heavy m_A . We set $2m_{\tilde{t}_1} = 1200$ GeV $\ll m_A$. In this case, we simply remove the s -pole contribution. Note that in this limiting case, the two-loop contribution of the pseudoscalar boson A^0 to the eEDM vanishes as well.

Note that we do not choose m_A very close to $m_{\tilde{\eta}}$ in case (1), because for such a low m_A the contribution to the eEDM would be large. In Fig. 2, we show the branching ratios of the stoponium in upper panels with the corresponding predictions for the eEDM in the lower panels, where we have chosen the heavier stop mass $m_{\tilde{t}_2}$ to be 1 TeV and $m_A = 1.5$ TeV. For simplicity we have also chosen $\text{Re}[\mu^* e^{-i\delta_u}] = 0$. We note that the partial width into Zh depends on $\text{Im}[\mu^* e^{-i\delta_u}]$, as indicated in Eq. (7), and the eEDM is also proportional to $\text{Im}[\mu^* e^{-i\delta_u}]$, as shown in Eq. (13). Therefore, we cannot choose the parameter $\text{Im}[\mu^* e^{-i\delta_u}]$ arbitrarily large. It is clear from the lower panels in Fig. 2 that $\text{Im}[\mu^* e^{-i\delta_u}] = 200$ GeV is the largest allowed value without violating the constraint of eEDM under the set of other input parameters shown in the figure caption. The branching ratio in Zh is also small, and of order 10^{-3} only.

An interesting observation can be found in Eq. (13) that when the heavier stop mass is indeed close to the lightest stop mass, a significant cancellation between these two contributions is possible. In Fig. 3, we show the branching ratios of the stoponium and the corresponding predictions for the eEDM with $m_{\tilde{t}_2} = 650$ GeV and heavier $m_A = 2.5$ TeV (case 2). The parameter $\text{Im}[\mu^* e^{-i\delta_u}]$ can be chosen as large as 2000 GeV without violating the constraint of eEDM. With such a large $\text{Im}[\mu^* e^{-i\delta_u}]$ the branching ratio into Zh can be as large as 10%. With such a large branching ratio, the stoponium decay into Zh now becomes very interesting and detectable.

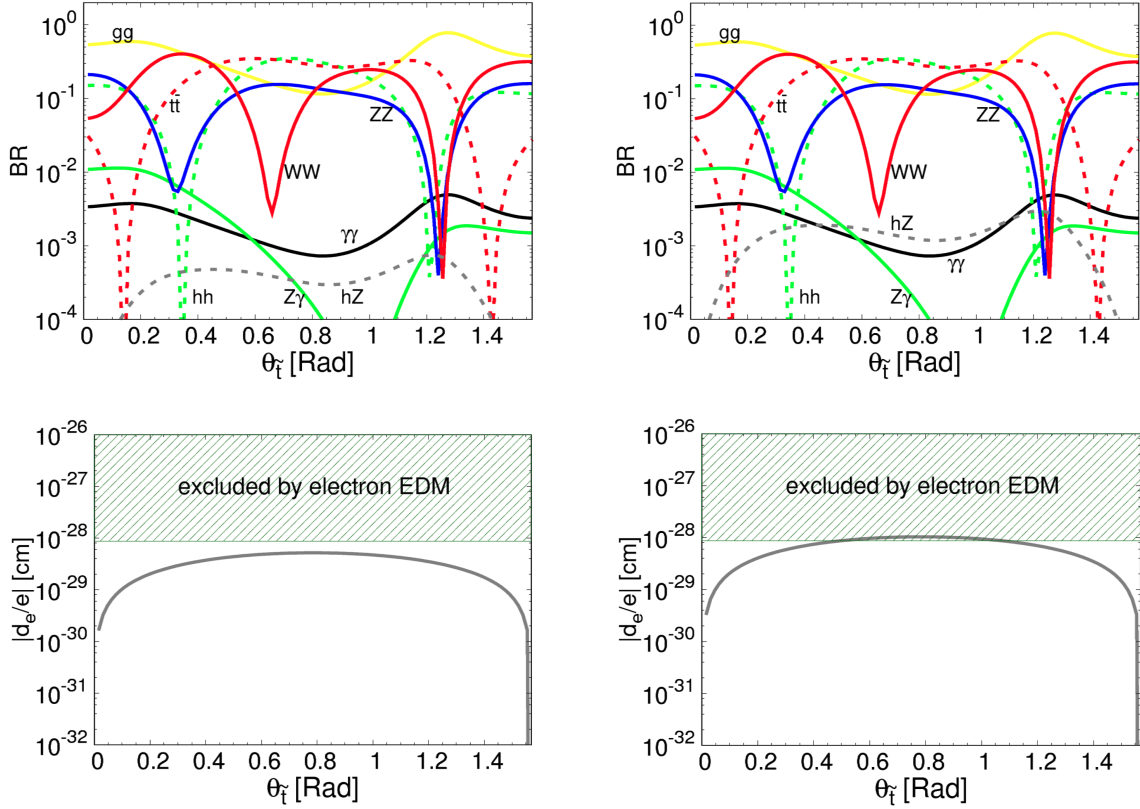


FIG. 2. Upper panels show the branching ratios of the stoponium with the corresponding predictions for the predicted eEDM from the two-loop Barr-Zee diagrams shown in the lower panels. We set $\delta_u = 0$, and μ purely imaginary, i.e. $\text{Re}[\mu^* e^{-i\delta_u}] = 0$. In the left (right) panel, we choose $\text{Im}[\mu^* e^{-i\delta_u}] = 100$ (200) GeV. For all panels we fix $m_{\tilde{t}_1} = 600$ GeV, $m_{\tilde{t}_2} = 1$ TeV, $m_{\tilde{g}} = 2$ TeV, $\tan\beta = 10$, $\cos(\beta - \alpha) = 0.1$, $m_h = 125$ GeV, $m_{H,A} = 1.5$ TeV, and vary $\theta_{\tilde{t}} \subseteq [0, \frac{\pi}{2}]$. We include the binding energy effect in the stoponium mass, $m_{\tilde{\eta}} = 1195$ GeV.

In the extreme case of case (3), the mass of the pseudoscalar A^0 is set to be very heavy. Practically, we ignore the term involving the A^0 exchange. We show in Fig. 4 the branching ratios for the stoponium with $m_{\tilde{t}_1} = 600$ GeV and $m_{\tilde{t}_2} = 1000$ GeV, except for the lower-right panel where $m_{\tilde{t}_2} = 650$ GeV. Since there are no more A^0 contribution to the eEDM, we can set the parameter $\text{Im}[\mu^* e^{-i\delta_u}]$ large enough to achieve a dominant branching ratio for the Zh mode. We have chosen $\text{Im}[\mu^* e^{-i\delta_u}] = 100, 200, 5000,$ and 5000 GeV, respectively. Note that increasing $\text{Im}[\mu^* e^{-i\delta_u}]$ will also increase the hh mode, because the partial width $\Gamma(\tilde{\eta} \rightarrow hh) \propto |y_{\tilde{t}_1 \tilde{t}_2}^h|^2$, and $\Gamma(\text{stoponium} \rightarrow hZ) \propto \text{Im}[y_{\tilde{t}_1 \tilde{t}_2}^h]$. In the most favorable case, the branching ratio into Zh can be of order $O(0.5)$, as indicated in the lower-right panel.

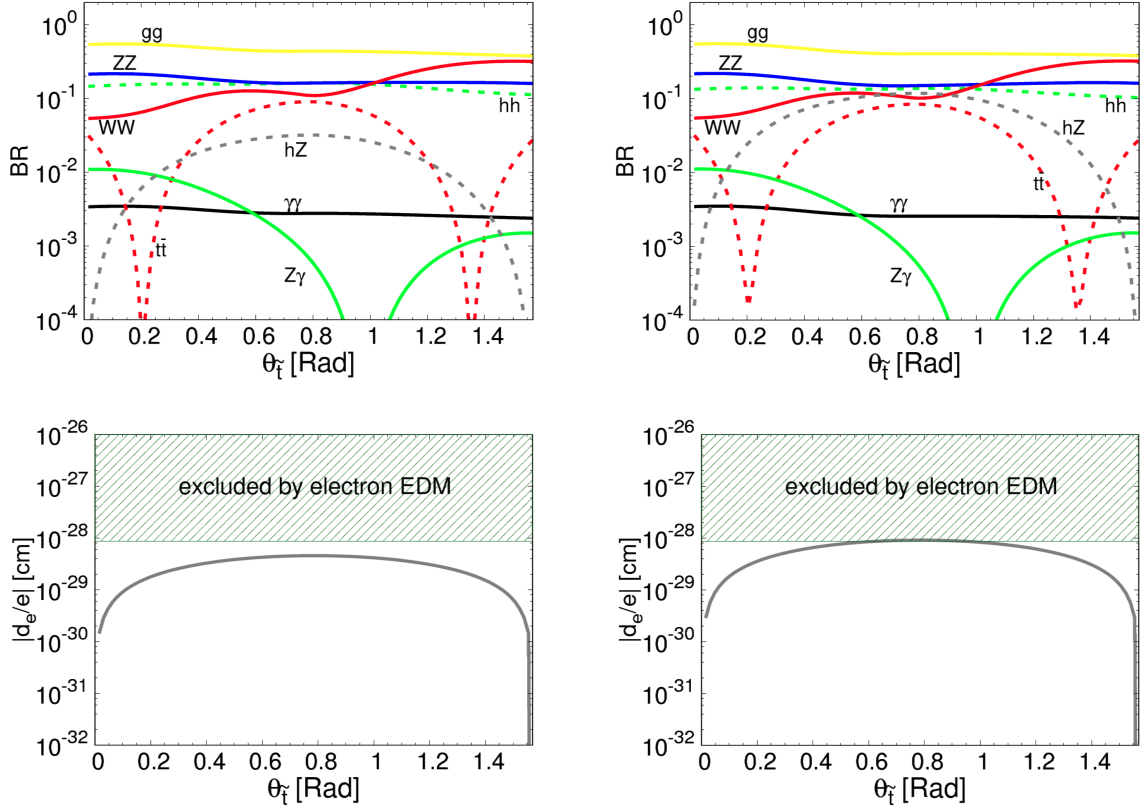


FIG. 3. Upper panels show the branching ratios of the stoponium with the corresponding predictions for the predicted eEDM from the two-loop Barr-Zee diagrams shown in the lower panels. We set $\delta_u = 0$, and μ purely imaginary, i.e. $\text{Re}[\mu^* e^{-i\delta_u}] = 0$. In contrast to Fig. 2, here we set $m_{H,A} = 2.5$ TeV, $m_{\tilde{t}_2} = 650$ GeV, and $\text{Im}[\mu^* e^{-i\delta_u}] = 1000$ (2000) GeV for the left (right) panels. The other input parameters are the same as Fig. 2.

IV. OBSERVABILITY AT THE LHC

The leading order(LO) production process for $\tilde{\eta}$ at LHC is through the gluon-gluon fusion, $gg \rightarrow \tilde{t}_1 \tilde{t}_1^*$. The cross section can be expressed in term of its gluonic decay width as [7]

$$\sigma(pp \rightarrow \tilde{\eta}) = \frac{\pi^2}{8m_{\tilde{\eta}}^3} \Gamma(\tilde{t}_1 \tilde{t}_1^* \rightarrow gg) \int_{\tau}^1 dx \frac{\tau}{x} g(x, Q) g(\tau/x, Q), \quad (15)$$

where $g(x, Q)$ is the gluon parton distribution function, and $\tau \equiv m_{\tilde{\eta}}^2/s$ with the center of mass energy of pp collision \sqrt{s} . For the parton distribution function, we used CTEQ6 [23] with the factorization scale $Q = m_{\tilde{\eta}}$. The K-factor, which is the ratio between the next leading order (NLO) and the LO cross sections, we take a reasonable value about 1.4. For

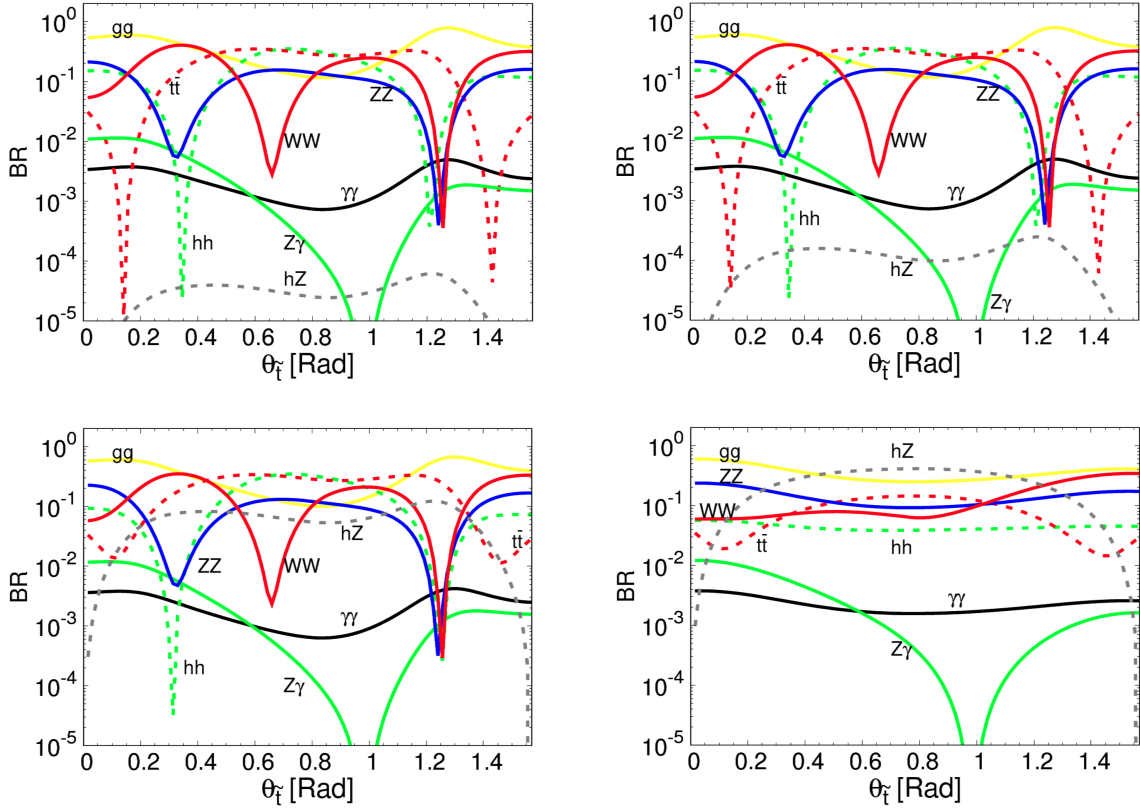


FIG. 4. In this extreme case of $m_A \rightarrow \infty$ the contribution to eEDM vanishes. Here we show the branching ratios of the stoponium for $m_{\tilde{t}_1} = 600$ GeV. The other relevant parameters are $m_{\tilde{t}_2} = 1$ TeV in the upper-left, upper-right, and lower-left panels, while $m_{\tilde{t}_2} = 650$ GeV in the lower-right panel. The $\text{Im}[\mu^* e^{-i\delta_u}] = 100, 200, 5000,$ and 5000 GeV, respectively. The other parameters are the same as in Fig. 2.

more detailed NLO calculation, we refer to Ref. [14]. At NLO, we obtain the production cross section for $m_{\tilde{\eta}} \simeq 1.2$ TeV at the LHC of $\sqrt{s} = 13$ TeV.

$$\sigma(pp \rightarrow \tilde{\eta}) \simeq 1 \text{ [fb]}. \quad (16)$$

The Zh decay mode of the stoponium can be searched for via $h \rightarrow b\bar{b}$ and $Z \rightarrow \ell^+\ell^-$ or $Z \rightarrow jj$. At the LHC, such searches have been performed [24–27], in which hadronic or leptonic modes of the Z boson and $b\bar{b}$ mode of the Higgs boson have been used. It is clear that the leptonic mode of the Z boson is clean but suffers from a small branching ratio. The hadronic mode of Z boson was believed to be suffered from large QCD background. Nevertheless, with the advance of various boosted-jet techniques the hadronic decays of the

Z boson and h can be performed with reasonable success. Since the stoponium is rather heavy $\sim 1.2 - 1.5$ TeV here, the Z boson and the Higgs boson are very boosted with $p_T \sim 0.6 - 0.75$ TeV. The opening angle between the decay products of the Z or the Higgs boson is $\sim 2M/p_T \sim 0.3 - 0.5$. This is in the right ballpark for excellent detectability of boosted jets in contrast to the conventional QCD background.

The recent search for $pp \rightarrow X \rightarrow Zh \rightarrow jjb\bar{b}$ performed by ATLAS[24] at the LHC gave an upper limit on $\sigma(pp \rightarrow X \rightarrow Zh) \times B(h \rightarrow b\bar{b} + c\bar{c}) < 20 - 30$ fb around the resonance mass $1.2 - 1.5$ TeV. On the other hand, the search $pp \rightarrow X \rightarrow Zh \rightarrow \ell^+\ell^-b\bar{b}$ was also performed [26]. The upper limit on $\sigma(pp \rightarrow X \rightarrow Zh) \times B(h \rightarrow b\bar{b} + c\bar{c}) < 10$ fb. Note that these searches were designated for vector resonances. In the same paper, they also gave $\sigma(pp \rightarrow A \rightarrow Zh) \times B(h \rightarrow b\bar{b}) < 10$ fb for $m_A \approx 1.2$ TeV. Therefore, the production cross section of the stoponium times the branching ratio into Zh is well below the current limits at the LHC.

With a project luminosity of 300 fb^{-1} at the end of Run II, we can expect about 15 events for $\tilde{\eta} \rightarrow Zh \rightarrow (jj, \ell\ell) + b\bar{b}$ for an optimistic branching ratio $B(\tilde{\eta} \rightarrow Zh) \sim 10\%$. We emphasize again that in CP -conserving case the stoponium would not decay into Zh , yet a small branching ratio into Zh would signal a violation of CP symmetry.

V. CONCLUSIONS

We have demonstrated that the decay mode of the ground state of the stoponium, $\tilde{\eta} \rightarrow Zh$, can have a dominant or significant branching ratio if we choose suitable CP violating mixing in the stop sector, which is still allowed by the eEDM measurement. Observation of such a decay mode of the stoponium is a clean signal of CP violation. The detailed phenomenology will be investigated in a separate analysis.

Our framework for the decay mode Zh from the scalar pair in the ground state can be extended to other models that have fundamental colored scalar bosons, such as the technipion[28] or the colored octet Higgs[29].

We offer a few comments before closing.

1. Both the partial width of $\tilde{\eta} \rightarrow Zh$ and eEDM increase with increase in the parameter $\text{Im}[\mu^* e^{-i\delta_u}]$. Therefore, we cannot make it arbitrarily large. When $m_A = 1.5$ TeV and $m_{\tilde{t}_1} = 600$ GeV, $\text{Im}[\mu^* e^{-i\delta_u}]$ can only be $100 - 200$ GeV.

2. The A^0 contribution would be suppressed with increases in m_A . Further suppression can be achieved with a smaller mass difference between $m_{\tilde{t}_1}$ and $m_{\tilde{t}_2}$. For $m_{\tilde{t}_1} = 600$ GeV and $m_{\tilde{t}_2} = 650$ GeV, and $m_A = 2.5$ TeV, the parameter $\text{Im}[\mu^* e^{-i\delta_u}]$ can be as large as 2000 GeV. The branching ratio for Zh can be enhanced to about 0.1.
3. In the extreme case of very heavy m_A , the A^0 contribution to eEDM vanished. Thus, we can choose a very large $\text{Im}[\mu^* e^{-i\delta_u}]$ such that the branching ratio into Zh can be of order $O(0.5)$.
4. There are other contributions to the eEDM from 1-loop diagrams in supersymmetric models, such as chargino-selectron loop and neutralino-sneutrino loop, and other 2-loop diagrams such as Barr-Zee diagrams with chargino, neutralino, stau, etc. Here in this work we only focus on a particular contribution from A^0 . In principle, we can allow some level of cancellation from other contributions, such that the sole contribution from A^0 may be over the current constraint. In such a case, the parameter $\text{Im}[\mu^* e^{-i\delta_u}]$ could be chosen a larger value and the branching ration into Zh could increase.

VI. ACKNOWLEDGMENTS

W.-Y. K. and P.-Y. T. thank the National Center of Theoretical Sciences and Academia Sinica, Taiwan, R.O.C. for hospitality. This research was supported in parts by the Ministry of Science and Technology (MOST) of Taiwan under Grant Nos. MOST-105-2112-M-007-028-MY3, and by the World Premier International Research Center Initiative (WPI), MEXT, Japan.

-
- [1] . Aad *et al.* [ATLAS Collaboration], “Observation of a new particle in the search for the Standard Model Higgs boson with the ATLAS detector at the LHC,” Phys. Lett. B **716**, 1 (2012) [arXiv:1207.7214 [hep-ex]]; S. Chatrchyan *et al.* [CMS Collaboration], “Observation of a new boson at a mass of 125 GeV with the CMS experiment at the LHC,” Phys. Lett. B **716**, 30 (2012) [arXiv:1207.7235 [hep-ex]].
- [2] M. Aaboud *et al.* [ATLAS Collaboration], [arXiv:1711.11520 [hep-ex]]. A. M. Sirunyan *et al.* [CMS Collaboration], Phys. Rev. D **97**, no. 3, 032009 (2018), [arXiv:1711.00752 [hep-ex]].

- [3] V. D. Barger and W. Y. Keung, Phys. Lett. B **211**, 355 (1988). doi:10.1016/0370-2693(88)90915-X
- [4] H. Inazawa and T. Morii, KOBE-FHD-93-06.
- [5] M. Drees and M. M. Nojiri, Phys. Rev. Lett. **72**, 2324 (1994) doi:10.1103/PhysRevLett.72.2324 [hep-ph/9310209].
- [6] M. J. Herrero, A. Mendez and T. G. Rizzo, Phys. Lett. B **200**, 205 (1988). doi:10.1016/0370-2693(88)91137-9
- [7] S. P. Martin, Phys. Rev. D **77**, 075002 (2008) doi:10.1103/PhysRevD.77.075002 [arXiv:0801.0237 [hep-ph]].
- [8] V. Barger, M. Ishida and W.-Y. Keung, Phys. Rev. Lett. **108**, 081804 (2012) doi:10.1103/PhysRevLett.108.081804 [arXiv:1110.2147 [hep-ph]].
- [9] C. Kim, A. Idilbi, T. Mehen and Y. W. Yoon, Phys. Rev. D **89**, no. 7, 075010 (2014) doi:10.1103/PhysRevD.89.075010 [arXiv:1401.1284 [hep-ph]].
- [10] N. Kumar and S. P. Martin, Phys. Rev. D **90**, no. 5, 055007 (2014) doi:10.1103/PhysRevD.90.055007 [arXiv:1404.0996 [hep-ph]].
- [11] B. Batell and S. Jung, JHEP **1507**, 061 (2015) doi:10.1007/JHEP07(2015)061 [arXiv:1504.01740 [hep-ph]].
- [12] G. H. Duan, L. Wu and R. Zheng, JHEP **1709**, 037 (2017), [arXiv:1706.07562 [hep-ph]].
- [13] S. P. Martin and J. E. Younkin, Phys. Rev. D **80**, 035026 (2009) doi:10.1103/PhysRevD.80.035026 [arXiv:0901.4318 [hep-ph]].
- [14] J. E. Younkin and S. P. Martin, Phys. Rev. D **81**, 055006 (2010) doi:10.1103/PhysRevD.81.055006 [arXiv:0912.4813 [hep-ph]].
- [15] S. Kim, Phys. Rev. D **92**, no. 9, 094505 (2015) doi:10.1103/PhysRevD.92.094505 [arXiv:1508.07080 [hep-lat]].
- [16] G. T. Bodwin, H. S. Chung and C. E. M. Wagner, Phys. Rev. D **95**, no. 1, 015013 (2017) doi:10.1103/PhysRevD.95.015013 [arXiv:1609.04831 [hep-ph]].
- [17] W. Y. Keung, I. Low and Y. Zhang, Phys. Rev. D **96**, no. 1, 015008 (2017), [arXiv:1703.02977 [hep-ph]]
- [18] J. Baron *et al.* [ACME Collaboration], Science **343**, 269 (2014), [arXiv:1310.7534 [physics.atom-ph]].

- [19] D. Chang, W. Y. Keung and A. Pilaftsis, Phys. Rev. Lett. **82**, 900 (1999) Erratum: [Phys. Rev. Lett. **83**, 3972 (1999)] doi:10.1103/PhysRevLett.83.3972, 10.1103/PhysRevLett.82.900 [hep-ph/9811202].
- [20] T. Ibrahim and P. Nath, Phys. Rev. D **58**, 111301 (1998) Erratum: [Phys. Rev. D **60**, 099902 (1999)] doi:10.1103/PhysRevD.60.099902, 10.1103/PhysRevD.58.111301 [hep-ph/9807501].
- [21] K. Cheung, J. S. Lee, E. Senaha and P. Y. Tseng, JHEP **1406**, 149 (2014) doi:10.1007/JHEP06(2014)149 [arXiv:1403.4775 [hep-ph]].
- [22] L. Bian, T. Liu and J. Shu, Phys. Rev. Lett. **115**, 021801 (2015), [arXiv:1411.6695 [hep-ph]].
- [23] J. Pumplin, D. R. Stump, J. Huston, H. L. Lai, P. M. Nadolsky and W. K. Tung, JHEP **0207**, 012 (2002) [hep-ph/0201195].
- [24] M. Aaboud *et al.* [ATLAS Collaboration], Phys. Lett. B **774**, 494 (2017) doi:10.1016/j.physletb.2017.09.066 [arXiv:1707.06958 [hep-ex]].
- [25] CMS Collaboration [CMS Collaboration], CMS-PAS-B2G-17-004.
- [26] M. Aaboud *et al.* [ATLAS Collaboration], [arXiv:1712.06518 [hep-ex]].
- [27] M. Aaboud *et al.* [ATLAS Collaboration], arXiv:1804.01126 [hep-ex].
- [28] V. D. Barger and W. Y. Keung, Phys. Lett. B **185**, 431 (1987). doi:10.1016/0370-2693(87)91030-6
- [29] M. I. Gresham and M. B. Wise, Phys. Rev. D **76**, 075003 (2007) doi:10.1103/PhysRevD.76.075003 [arXiv:0706.0909 [hep-ph]].